UVicSPACE: Research & Learning Repository

University of Victoria

Faculty of Science

Faculty Publications

This is a post-review version of the following article:

The role of sedimentation history and lithology on fluid flow and reactions in off-axis hydrothermal systems: A perspective from the Troodos ophiolite

K.M. Gillis, L.A. Coogan & C. Brant

2015

The final published version of this article can be found at:

https://doi.org/10.1016/j.chemgeo.2015.09.006

Citation for this paper:

Gillis, K.M., Coogan, L.A. & Brant, C. (2015). The role of sedimentation history and lithology on fluid flow and reactions in off-axis hydrothermal systems: A perspective from the Troodos ophiolite. *Chemical Geology*, 414, 84-94.
https://doi.org/10.1016/j.chemgeo.2015.09.006

Accepted Manuscript

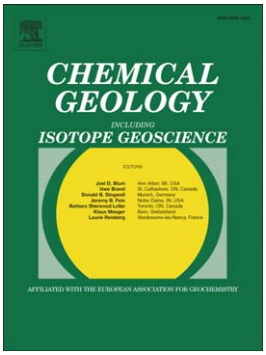

The role of sedimentation history and lithology on fluid flow and reactions in off-axis hydrothermal systems: A perspective from the Troodos ophiolite

K.M. Gillis, L.A. Coogan, C. Brant

PII: S0009-2541(15)30027-9
DOI: doi: 10.1016/j.chemgeo.2015.09.006
Reference: CHEMGE 17689

To appear in: *Chemical Geology*

Received date: 16 April 2015
Revised date: 19 August 2015
Accepted date: 5 September 2015

Please cite this article as: Gillis, K.M., Coogan, L.A., Brant, C., The role of sedimentation history and lithology on fluid flow and reactions in off-axis hydrothermal systems: A perspective from the Troodos ophiolite, *Chemical Geology* (2015), doi: 10.1016/j.chemgeo.2015.09.006

This is a PDF file of an unedited manuscript that has been accepted for publication. As a service to our customers we are providing this early version of the manuscript. The manuscript will undergo copyediting, typesetting, and review of the resulting proof before it is published in its final form. Please note that during the production process errors may be discovered which could affect the content, and all legal disclaimers that apply to the journal pertain.

ACCEPTED MANUSCRIPT

The role of sedimentation history and lithology on fluid flow and reactions in off-axis hydrothermal systems: A perspective from the Troodos ophiolite

K.M. Gillis[1,*], L.A. Coogan[1], and C. Brant[1]

[1] School of Earth and Ocean Sciences, University of Victoria, Victoria, BC, Canada

* Corresponding author, kgillis@uvic.ca, phone: 1-250-472-4023, fax: 1-250-721-6200

Key words: Ocean crust, off-axis, hydrothermal system, Li isotopes, Sr isotopes, Troodos ophiolite

Revised manuscript submitted to Chemical Geology 19 August 2015

ACCEPTED MANUSCRIPT

ACCEPTED MANUSCRIPT

Abstract

Off-axis hydrothermal systems are thought to carry globally significant chemical fluxes but different ocean crust sections show widely differing extents of alteration making the quantification of these fluxes complex. With the aim of better understanding the origin of this diversity in alteration extent we have studied two sections of the lava pile in the Troodos ophiolite with distinct sedimentation history and volcanic architecture. The Akaki section is dominated by pillow lavas and the oldest sediments overlying the crust are ~20 Myr younger than the ophiolite. Here there is a 300 m thick zone at the top of the lavas that is enriched in CO_2 and alkali elements, and has high $^{87}Sr/^{86}Sr$ and δ^7Li. These features indicate extensive chemical exchange with seawater. In contrast to the Akaki area, the Onophrious section is dominated by sheet flows and the oldest sediments are of the same age as the ophiolite. Here the CO_2 and alkali element enriched zone is much thinner (<100 m), is less enriched in these elements (e.g. by a factor of three for CO_2), and has lower $^{87}Sr/^{86}Sr$ and δ^7Li. The O-isotopic compositions of calcites from these CO_2- and alkali-enriched zones were precipitated from fluids with bottom water temperatures (~10°C). Maintaining such low temperatures to 300 m depth in the crust in the Akaki area suggests that this was a region of recharge. Below these CO_2- and alkali-enriched zones temperatures increase with depth such that calcite precipitation in the Onophrious area occurred at ~10°C higher temperature, at any given depth, than in the Akaki area. The increase in precipitation temperature with depth indicates poor thermal mixing within the crustal aquifer, likely due to laterally continuous sheet flows restricting the permeability. The chemical and thermal constraints suggest that both timing of the onset of sedimentation and volcanic architecture play important

ACCEPTED MANUSCRIPT

roles in controlling fluid and chemical fluxes. The same signal can be seen in drill core data from the modern ocean basins, with higher sedimentation rates leading to lower fluid fluxes and higher temperatures in the crustal aquifer.

1. Introduction

Low-temperature (10's of Celsius) hydrothermal circulation through the upper oceanic crust, away from the ridge axis, leads to globally significant fluxes of solutes into and out of the ocean (Mottl and Wheat, 1994; Staudigel, 2014). These off-axis hydrothermal systems carry about 25% of the global heat flow (Stein and Stein, 1994) and have fluid fluxes of the same order of magnitude as those from rivers (e.g. Fisher and Wheat, 2010). Changes in the alkalinity flux associated with rock alteration within ridge flank hydrothermal systems has been suggested to play an important, and maybe dominant, role in the long-term carbon cycle (Francois and Walker, 1992; Brady and Gislason, 1997; Gillis and Coogan, 2011; Coogan and Gillis, 2013). Additionally, changing bottom water temperature feeding off-axis systems and hence reaction rates within the crust, has been suggested to play a major role in controlling the secular variation in the Mg- and Sr-isotopic composition of seawater (Higgins and Schrag, 2015; Coogan and Dosso, 2015).

Fluid flow within the off-axis crustal aquifer (i.e. the lava pile) is driven by changes in fluid temperature, and hence density, due to extraction of lithospheric heat into the fluid. Since the heat budget is globally near uniform, and relatively well understood, the main unknown in modeling fluid flow comes from the distribution of

ACCEPTED MANUSCRIPT

permeability within the upper crust (e.g. Fisher and Becker, 2000). Two controls on permeability need to be considered: sediment cover and lava lithology.

Sediment deposited on top of the crust acts as an impermeable layer impeding the ingress of seawater into the crustal aquifer (e.g. Spinelli et al., 2004). Today, abyssal sedimentation rates vary globally so the ability of fluid to enter and exit the crust is expected to be quite variable. Over time a crustal section likely passes through three general stages of sediment cover. At very young ages, sediment is generally thin enough that fluid flow is not inhibited substantially. At intermediate ages, sediment fills topographic lows and fluids will enter and leave the crust through isolated outcrops (e.g. Fisher and Becker, 2000; Anderson et al., 2012). At older ages sediment forms a near impermeable blanket vastly decreasing fluid exchange between the lavas and ocean.

The accretion of the lava pile leads to large spatial variations in permeability on a range of scales (Fisher, 1998). Lavas are commonly described as sheet (or massive) flows, pillow flows and breccias (or hyaloclastites) with large differences in permeability (Gillis and Sapp, 1997; Bach et al., 2004). Faults are also likely to play an important, but poorly understood, role in crustal permeability, both producing local high permeability pathways and offsetting high permeability layers, hence decreasing large-scale permeability (Fisher, 1998). Different crustal sections will have different permeability structures reflective of their particular lithologic stratigraphy and tectonic disruption.

Here we present a comparison of the compositions of two crustal sections of the Troodos ophiolite with differing sedimentation history and lava stratigraphy. The Troodos ophiolite was selected for this work as it has the best preservation of the low-temperature, off-axis hydrothermal alteration of any ophiolite and because the exposure

ACCEPTED MANUSCRIPT

and preservation of the upper crustal sequences is exquisite. The Troodos ophiolite formed in the Cretaceous (91.6 ± 1.4 Myr; Mukasa and Ludden, 1987) above a subduction zone (e.g. Miyashiro, 1973) but has an off-axis hydrothermal alteration history very similar to that of modern oceanic crust (e.g. Bednarz and Schmincke, 1989; Gillis and Robinson, 1988). We show that the bulk-rock geochemistry, including Sr- and Li-isotopic compositions, of the two studied crustal sections differ substantially as does the temperature of calcite precipitation. These differences are interpreted as recording the importance of crustal permeability on off-axis hydrothermal fluxes. Comparison with data from a global suite of drill cores from the modern ocean basins suggests the same controls in the modern ocean basins, as well as demonstrating the importance of the history of sedimentation.

2. Materials and Methods

2.1 Field relationships

Two well-exposed lava sections in the Troodos ophiolite were selected for study based on differing sedimentation history and lava stratigraphy. The two study areas are ~7.5 km apart along the northern flank of the ophiolite (Fig. 1). The Akaki section was the location of extensive study in the 1980's (e.g. Rautenschlein et al., 1985; Gillis and Robinson, 1990) and was the location of the International Crustal Research Drilling Group (ICRDG) drill holes CY1 and CY1A. These holes were offset from one another (Fig. 1a) with the aim of stacking them to produce a complete section through the lavas and upper sheeted dikes (Robinson, 1991). Samples from these drill cores were largely used in this study because previous work on these cores provides context for this study.

ACCEPTED MANUSCRIPT

The Onophrious section, to the east of Akaki, is well-exposed along the Onophrious river and surface samples were collected here (Fig. 1b).

In the Akaki area, mapping along the lava–sediment interface shows that the lava section is overlain by chalky limestones of the Late Cretaceous to Tertiary Lefkara formation (Bear, 1960) and the contact is very planar dipping about 7°N with only very subdued (probably <10 m) paleoseafloor topography over >1 km along strike (Fig. 1a). The average dip of the sediments is somewhat steeper than that of the lava–sediment interface, 20° towards 355. This difference is most simply explained by deposition of the sediments onto an initially gently south sloping seafloor (in the modern reference frame). Subsequent northward rotation of this portion of the ophiolite, about a horizontal east-west axis, would be consistent with the data. We take the average sediment dip (20°) to reflect the average dip of the crust in this area when determining depths within the crust both for the surface and drill core samples; using dips between 10 and 30° would lead to <8% change in sample depths. Both surface geology and the drill cores show that the upper 300 m of the lava section at Akaki is dominated by pillows and breccias, with an increasing abundance of sheet flows with depth (Fig. 1a). Pillows still make up ~40% of the lower ~300 m of the section, where pillows and sheets are intermixed on a scale of meters to 10's of meters.

In the Onophrious area the lavas are overlain by 5-10 m of variably silicified umbers, radiolarian shales and marls of the Late Cretaceous Perapedhi formation, the oldest sedimentary unit overlying the ophiolite (Bear, 1960). The Perapedhi formation is overlain, in turn, by chalky limestones of the Lefkara formation similar to those found directly overlying the lavas in the Akaki area. The sedimentation rate for the Lefkara

ACCEPTED MANUSCRIPT

formation exposed along the northern flank of the ophiolite is not well constrained, but is estimated at ≤1 m Myr^{-1} (Bear, 1960). The umbers and silicic sediments are associated with a ~50 m deep and ~750 m wide NS trending (roughly dike parallel) depression in the lava-sediment interface (Fig. 1b). This is interpreted as a paleo-seafloor topographic low, most likely a fault-bound graben, in which the oldest sediments preferentially accumulated prior to the onset of carbonate sedimentation (or at least calcite preservation). Thus, sediment accumulation commenced significantly earlier (on the order of 20-30 Myr) in the Onophrious than Akaki area. The average dip of the lava-sediment interface in this area is difficult to determine from the map pattern due to the paleo-seafloor topographic depression and poor exposure to the east of this. The average dip in the sediments filling the 'graben' is 17° toward 015, and it is assumed that the section is tilted by this amount when determining depths below the seafloor. The uppermost 50–60 m of the lavas in the Onophrious section are pillows and the remaining section is composed of sheet flows with one thin interval of pillows (Fig. 1b). This stratigraphy contrasts starkly with the much more abundant pillows in the Akaki section at an equivalent depth in the crust suggesting that the permeability structure of these sections differed substantially.

The lavas from the two locations are tholeiitic and range in composition from basaltic andesite to dacite (Appendix B; Rautenschlein et al., 1985; Bednarz and Schmincke, 1989; Regelous et al., 2014). In both areas, the lava sequence is variably altered to assemblages of low temperature clay minerals, zeolites, and calcites (this study; Gillis and Robinson, 1988; 1990). The characteristic secondary mineral assemblage of a given outcrop depends on its depth within the lava pile and the dominant lava

ACCEPTED MANUSCRIPT

morphology (i.e., pillows, flows, breccias; Gillis and Robinson, 1990). The uppermost lavas are characterized by pervasive alteration and void in-filling, saponite and Al-saponite are the dominant clay minerals, adularia commonly replaces igneous plagioclase and calcite is abundant. This style of alteration typifies the upper ~300 m of the lava section at Akaki and the upper ~100 m at Onophrious. The underlying lavas in both sections are characterized by a wide range in the pervasiveness of alteration and extent of void-infilling, with fresh glass locally preserved. Saponite and celadonite are the dominant clay minerals and calcite is less abundant than in the upper lavas.

2.2 Sample suite and analytical methods

The altered lavas sampled from surface outcrops and drillcore include pillows sheet flows, and hyaloclasties that are comprised of varying proportions of void-filling secondary minerals, altered crystalline rock and altered glas s (e.g., Gillis and Sapp, 1997). To ensure this variability was accounted for in our sample suite, both altered margins and interiors of pillows and sheet flows were sampled (Supplementary Table 1). Margin samples include variably altered glass, secondary minerals cementing the altered glass, and the adjacent altered crystalline rock whereas the interior samples include altered crystalline rock and the secondary minerals filling veins and vesicles. The specific proportions of each of these components were variable, as would be expected in heterogenous outcrops.

To assess whether a sample bias was introduced by using both surface and drillcore samples we rely on an previous study of the Akaki area (Gillis and Robinson, 1990; Gillis, 1987). This study showed that, at an equivalent depth below the sediment-lava interface, the composition and relative proportion of secondary minerals replacing

ACCEPTED MANUSCRIPT

pillows and sheet flows are comparable. As these secondary minerals lead to the compositional changes associated with alteration, we conclude that sample type does not introduce a bias in our comparisons between field areas.

Whole rock and calcite samples were selected to provide comparable depth profiles for the two study areas that display contrasting sedimentation histories and lithological make-up. At Akaki, published geochemical datasets for Holes CY1/1A (Gillis and Robinson, 1990; Gibson et al., 1991) were augmented by sampling representative sections from the drill cores and analyzing available whole rock powders for trace element abundances and Li- and Sr-isotope ratios. Published calcite compositions for samples from Holes CY1/1A were augmented by sampling calcite amygdules from surface exposures. Volcanic glass was separated from both drill core and surface samples. At Onophrious, surface samples of whole rocks (representative of the igneous and alteration characteristics), calcite amygdules and volcanic glass were collected. Analytical methods for the whole rock major, trace element, and Sr- and Li-isotope analysis; glass and clay mineral major and trace element analysis; and calcite O- and Sr-isotope analysis are given in Appendix A. Tabulated data is provided in Appendix B.

3. Results

3.1 Whole-rock major and trace element compositions

The lavas in both study areas are enriched in fluid-mobile elements, as would be expected for submarine lavas altered at low temperatures (e.g. Hart and Staudigel, 1982). The upper lavas are CO_2-enriched, due to the precipitation of calcite in voids and local replacement of primary phases. The thickness of the CO_2-enriched zone is ~300 m at Akaki and <100 m at Onophrious, with >3 times the level of enrichment at Akaki (upper

ACCEPTED MANUSCRIPT

300 m average 4.5 wt%) relative to Onophrious (upper 100 m average 1.3 wt%; Fig. 2a). Below these upper enriched zones, CO_2 decreases markedly to <1 wt% (Akaki average 0.9 wt%; Onophrious average 0.2 wt%). The exact thickness of the CO_2-enriched region in the Onophrious area is unclear due to a sampling gap between the base of the pillow lavas at 65 m (CO_2-enriched) and the next sample at 100 m (a CO_2-poor sheet flow; Fig. 1b). Thus, throughout we refer to the upper enriched zone as being <100 m thick.

The alkali elements Li, K and Rb follow similar depth trends to CO_2, with more enrichment, over a larger depth interval, in the Akaki than Onophrious section; all elements are substantially enriched relative to fresh glass (Fig. 2). Comparison of the K_2O contents of the altered rocks with average fresh glass shows that the upper enriched zone at Akaki (~3.1 wt%) is ~14 times and at Onophrious (~2.4 wt%) is ~11 times enriched in K_2O relative to average fresh glass (Supplementary Table 1), with the underlying lavas (~0.6 wt% K_2O) at both locations being ~3 times enriched (Fig. 2b). Lavas in the enriched zones at Akaki and Onophrious are ~6 and ~4 times more enriched in Rb (average Rb concentrations of 27 and 20 ppm), respectively, with the underlying lavas at both locations containing about twice the Rb of average glass (Fig. 2c). Finally, lavas in the enriched zone at Akaki and Onophrious are ~10 and ~8 times enriched in Li (average Li concentrations of 46 and 35 ppm) relative to average volcanic glass, respectively (Fig. 2d). In contrast to K_2O and Rb, the deeper lavas in the Akaki section are still strongly enriched in Li (~5x) but the deeper samples are not substantially enriched in Li in the Onophrious section (Fig. 2d).

Determining the reactive fluid flux through the crustal sections requires making assumptions about the composition of Cretaceous seawater, and the fraction of each

ACCEPTED MANUSCRIPT

element stripped from the fluid and added to the crust, but these assumptions can be largely circumvented if relative fluid fluxes are determined. Because the upper enriched zone for the alkali elements and CO_2 in the Akaki section is both thicker and more strongly enriched, the total addition of these elements to the crust is far greater in the Akaki than Onophrious area. To numerically compare these differences, the mass of each species added to the crust, assuming no change in composition outside of the depth ranges shown in Figure 2 (600 m for Akaki and 300 m for Onophrious), was calculated using the 50 m interval average compositions shown in Figure 2 and the average glass composition as the protolith composition (Supplementary Table 2)(zero for CO_2); a density of 2700 kg m^{-3} was assumed. The Akaki section contains ~7 times more CO_2 (~$40x10^3$ kg m^{-2}) than the Onophrious section (~$5.4x10^3$ kg m^{-2}) and ~3.5-4 times more Li (44 v 11 kg m^{-2}), K_2O (27 v $8x10^3$ kg m^{-2}) and Rb (23 v 7 kg m^{-2}). The alkali elements Li, K and Rb are hosted in different phases in altered ocean crust (e.g. K in adularia and celadonite and Li in smectite; Staudigel et al., 1986; Staudigel and Gillis, 1990; see below). Thus, the very similar relative enrichments of Li, K and Rb in the Akaki section relative to the Onophrious section suggests that the flux of 'fresh reactive fluid', rather than mineralogy, is the primary control on the abundance of these elements. We use the term 'fresh reactive fluid' to indicate fluid that has a seawater-like composition to differentiate this from a total fluid flux that could include an unlimited amount of fluid that has equilibrated with the crust in a different place and leaves no geochemical signature.

In summary, the upper ~300 m of the Akaki section and <100 m of the Onophrious section are enriched in CO_2, K_2O, Rb and Li, with greater enrichment at

ACCEPTED MANUSCRIPT

Akaki. Beneath these upper enriched zones, the lavas are significantly less enriched, with equivalent levels for K_2O and Rb at both locations, but lower levels of CO_2 and Li at Onophrious. As will be discussed below, it is significant that at an equivalent depth, the lavas at Akaki are more enriched in all the elements considered here than at Onophrious.

3.2 Whole-rock strontium isotope ratios

The strontium isotopic compositions of whole rock samples provide information about the amount of Sr exchange between the upper crust and seawater-derived hydrothermal fluids. The Sr-isotopic compositions of fresh glass and fresh gabbro suggest an initial magma $^{87}Sr/^{86}Sr$ of ~0.7035 (Spooner et al., 1977; Rautenschlein et al., 1985). The age-corrected Sr-isotopic compositions of the altered lavas (see Appendix A for details) range from near the fresh rock value to almost the same as Late Cretaceous seawater (~0.7073, McArthur et al., 2001; Fig. 3a). Although $^{87}Sr/^{86}Sr$ decreases with depth at both locations, samples from the Akaki section have substantially higher $^{87}Sr/^{86}Sr$ than those from the Onophrious section at an equivalent depth (Fig. 3a). The range of Sr contents for samples with Sr-isotopic data (59 to 131 ppm) overlaps the range for fresh volcanic glass (62 to 110 ppm; Supplementary Table 2; Regelous et al., 2014) indicating that the Sr-isotopic compositions of the altered rocks generally record Sr-exchange during fluid-rock reaction, rather than simply Sr addition during mineral precipitation from seawater.

The Sr-isotopic compositions of calcite separates, which record the Sr-isotopic composition of the aquifer fluids, are generally slightly lower than contemporaneous seawater (see Section 3.4). Rock dissolution followed by precipitation of secondary minerals from the slightly modified (lower $^{87}Sr/^{86}Sr$) fluid can explain the Sr-isotopic

ACCEPTED MANUSCRIPT

composition of both the calcites and whole rock samples, with more extensive exchange in the Akaki section than the Onophrious section.

One way to quantify the more extensive fluid-rock exchange in the Akaki than the Onophrious section, indicated by higher $^{87}Sr/^{86}Sr$ values (Fig. 3a), is to calculate closed-system water-rock ratios. While the values calculated from such an approach generally do not reflect the true ratio of fluid to rock, the relative difference between the two areas provides insight into the differences between the fluid-rock reaction histories. Figure 3b shows that the average closed-system water-rock ratio is ~175 for the Akaki area and ~50 for the Onophrious area. This difference cannot simply reflect reaction of an evolved, rock-buffered aquifer fluid with the Onophrious section because the high $^{87}Sr/^{86}Sr$ of the calcites (Fig. 4b)(and other secondary phases, Staudigel et al., 1986; Staudigel and Gillis, 1990) demonstrate that low-temperature fluids did not become rock buffered. Thus, we interpret the difference in $^{87}Sr/^{86}Sr$ of the whole rock samples to record differences in the extent of reaction with the aquifer fluids. While calculated in a different way, making different assumptions (see caption to Fig. 3), the water-rock ratios are entirely consistent with the extent of enrichment derived from the alkali element contents of the two sections; i.e. the flux of 'fresh reactive fluid' was substantially larger (~3-4 times) in the Akaki than the Onophrious section.

3.3 Whole-rock lithium isotope ratios

Lithium isotopes are powerful tracers of low-temperature alteration of the oceanic crust. Lithium is taken up from seawater into low-temperature phases leading to a strong enrichment of Li in rocks altered at low temperatures (e.g. Chan et al., 1992, Fig. 2). There is a significant isotopic fractionation during alteration, such that ^{6}Li is

ACCEPTED MANUSCRIPT

preferentially incorporated into low-temperature minerals relative to the aqueous fluid. However, altered rocks are still shifted towards heavier δ^7Li because seawater is isotopically heavier than fresh lava. The expected fractionation between low-temperature alteration minerals and seawater is, on average, ~16‰, based on the correlation of δ^7Li and 1/Li in a series of dredged and drilled samples (Chan et al., 1992; Chan et al., 2002).

A complexity in using the Li-isotopic composition of our samples to track low-temperature alteration processes is that the Li-isotopic composition of seawater has changed over time (δ^7Li of modern seawater is ~31‰ and the lowest seawater δ^7Li in the last 65 Myr was 23‰; Misra and Froelich, 2012) and the isotopic composition of 90 Myr seawater is unknown. Additionally, the δ^7Li for fresh Troodos lavas is not known. However, lavas from other supra-subduction zone settings typically have δ^7Li between 0.9 and 7.4‰ (e.g. Tomascak et al., 2002; Magna et al., 2006), which is also within the range of mid-ocean ridge basalt (3.4 ± 1.4 ‰; Tomascak et al., 2008). Thus we assume a protolith composition also within this range.

The Li content of fresh glass from the Akaki and Onophrious areas ranges from 0.2 to 8 ppm (Supplementary Table 2; Regelous et al., 2014). All but two of the altered whole rock samples with Li-isotopic data show Li-enrichment (14–101 ppm) indicating that the Li budget in these samples is generally dominated by secondary minerals. The δ^7Li of the whole rock samples range from 7 to 12‰, falling between seawater and fresh rock values. Samples from the upper half of the Akaki section are slightly heavier (9.5–12‰) than both those from deeper in the lava section and all but one sample from the Onophrious section (7–9‰; Fig. 5a). Samples showing Li enrichment (>14 ppm) show a distinction between low K_2O (≤1.01 wt%) and high K_2O (1.56 to 5.95 wt%) samples,

ACCEPTED MANUSCRIPT

with the former having δ^7Li between 7 and 9‰ and the latter having δ^7Li between 9.5 and 12‰ (Fig. 5b). There are two exceptions to this general observation, both of these samples have low Li concentrations for which the contribution of magmatic Li may be important. Thus this ~3‰ difference between locations appears robust.

Two possible explanations for the variation in δ^7Li with depth in the Akaki section and between the two study areas are: (i) difference reactive fluid fluxes and (ii) different alteration temperatures and/or secondary mineral assemblages, leading to different bulk isotopic fractionation factors. If the extent of fluid-rock reaction was the only control on the Li-isotopic composition of the altered rocks we would expect to see a strong correlation between Li-content and δ^7Li, which is not the case. If temperature was the sole control on the fractionation factor for Li-isotope exchange between the fluid and rock then the rocks should be lightest (most fractionated from the fluid) at the top on the crust especially in the Akaki section (Fig. 4a), the inverse of what is observed. However, the difference in δ^7Li in the samples with high Li contents does appears to be, at least in part, linked to the bulk rock K-content (Fig. 5b) which largely reflects the abundance of high K secondary minerals. If this correlation is confirmed by future data, the simplest explanation would be smaller fractionation factor for the K-rich secondary mineral assemblages (celadonite-richer) than for the K-poor mineral assemblages (smectite-richer).

3.4 Calcite isotope geochemistry

The isotopic compositions of the calcite separates are indicative of aquifer fluid compositions, recording information about conditions at the time of precipitation (e.g.

ACCEPTED MANUSCRIPT

Coggon et al., 2010; Gillis and Coogan, 2011)(Supplementary Table 3). The $\delta^{18}O$ of calcite ranges from +24.8 to + 32.5‰ VSMOW; no difference was observed between samples collected from surface exposures versus drillcore at approximately equivalent depths. Formation temperatures calculated using the O-isotope thermometer of Friedman and O'Neil (1977), and assuming a Cretaceous seawater $\delta^{18}O$ of -1.0 ‰ (e.g. Veizer et al., 1999), are ~10°C in the upper 300 and 100 m at Akaki and Onophrious, respectively (Fig. 4a). These are similar to late Cretaceous bottom water (Huber et al., 2002) suggesting the fluids at these depths in the crust had not been substantially warmed by lithospheric heat. The calcite precipitation temperatures increase to ~35°C at greater depths in both locations (Fig. 4a). A significant observation, discussed below, is the systematically higher temperature (up to 10°C) at an equivalent depth at Onophrious relative to Akaki.

The Sr-isotopic composition of the calcite separates ranges from 0.70779 to 0.70673, and shows no systematic change with depth in either study area (Fig. 4b). If calcite is assumed to have precipitated from a fluid with an $^{87}Sr/^{86}Sr$ identical to seawater, comparison of its $^{87}Sr/^{86}Sr$ with the seawater Sr-isotope curve indicates that most calcite formed within 20 million years of crustal formation, with most of the Onophrious samples having $^{87}Sr/^{86}Sr$ close to that of 90 Myr seawater (Fig. 4b). This is because seawater became progressively more radiogenic from the late Cretaceous (e.g. McArthur et al., 2001). The timing of calcite precipitation proposed here, largely within 20 Myr of crustal formation, is consistent with quantitative modeling of a global dataset of $^{87}Sr/^{86}Sr$ for submarine, lava-hosted carbonates (Gillis and Coogan, 2011; Coogan and Dosso, 2015) and ages of other secondary minerals from the Troodos ophiolite (Staudigel et al.,

ACCEPTED MANUSCRIPT

1986; Gallahan and Duncan, 1994; Booij et al., 1995). If the basement fluids were modified by reactions with the lavas, adding unradiogenic basaltic Sr to the fluid prior to calcite precipitation, the carbonates could have formed somewhat later.

3.5 Clay Mineral Geochemistry

The K_2O, Rb and Li contents of clay minerals and altered glass (palagonite) from a subset of samples were determined to assess where these elements reside in the altered rocks (Supplementary Tables 4 and 5). The concentration of K_2O and Rb varies with clay type, with the highest concentrations found in celadonite and celadonite-saponite mixtures (Fig. 6a and b). The concentration of Li also varies with clay type, with the highest concentrations in saponite and saponite-chlorite mixtures (Fig. 6c). Lithium concentrations in the clay minerals show no correlation with the other alkali elements suggesting that its uptake is controlled by a different mechanism. Whilst a detailed analysis of what controls the uptake of these elements in clay minerals is out of the scope of this contribution, we note that cations with low hydration energies, such as K (-321 kJ/mol) and Rb (-296 kJ/mol), are preferentially incorporated into interlayer sites (e.g. Teppen and Miller, 2006). In contrast, the high hydration energy of Li (-515 kJ/mol) means it is unlikely to partition into interlayer sites, so other mechanisms need to be considered (e.g. Vigier et al., 2008).

Palagonite (altered volcanic glass) is enriched in K_2O, Rb and Li, similar to the clay minerals. Palagonites with high SiO_2, and low K_2O and Rb contents have the highest Li concentrations (>180 ppm) (Supplementary Table 5). Texturally, these yellowish brown to brown grains are fibro-palagonites, suggesting that incipient gel-palagonites have recrystallized to assemblages of mixed smectite minerals (e.g. Stroncik and

ACCEPTED MANUSCRIPT

Schmincke, 2001). This implies that as glass ages, it progressively takes up Li in environments that favour saponite formation over celadonite. This is consistent with our clay mineral data, such that the clays with the highest Li contents are saponites and saponite-chlorite mixtures.

4. Discussion

The bulk-rock compositions reported here suggest that the fluid flux was substantially (>3x) larger through the Akaki than the Onophrious crustal section (Fig. 2, 3). This difference in fluid flux is paralleled by differences in the thermal state of the crust during fluid-rock reaction as indicated by calcite precipitation temperatures (Fig. 4a). Further, the range of calcite Sr-isotopic compositions (Fig. 4b) suggests that calcite precipitation continued for a longer duration in the Akaki area than the Onophrious area. These regional variations must reflect differences in the hydrological regime in these two areas and correlate to clear differences in the timing of sedimentation and the volcanic architecture. Below the thermal evolution of these crustal sections is explored to better understand the hydrological implications. This work is then put in a global context by comparison with data from drill cores in the modern ocean basins.

4.1 Contrasting hydrological regimes in the Akaki and Onophrious sections

Calcite precipitation temperatures provide information about the thermal conditions during the time at which the crustal aquifer fluids were saturated in calcite. They are close to that of Cretaceous bottom water at the top of both sections, stay constant throughout the zone of CO_2 and alkali enrichment, and then increase with depth (Fig. 4a). As a starting point for interpreting the difference in calcite precipitation

ACCEPTED MANUSCRIPT

temperatures between the two sections, we assess the temperature distribution expected if there was no fluid flow. This can be estimated as a function of time after crustal formation based on a simple thermal conduction model given an estimate of the heat flow as a function of crustal age (taken from Stein and Stein, 1992) and an estimate of the sedimentation rate ($\leq$1 m Myr^{-1}; taken from Bear, 1960). We use the predicted heat flow value for 5 Ma lithosphere, as this is the age at which ~50% of carbonate has formed (e.g. Coogan and Dosso, 2015) and the average age for the formation of alkali-bearing secondary minerals (see above). However, the conductive geotherm is not dramatically different by 20 Myr (Fig. 4a). This conductive model constrains the maximum temperature limit within the crust, as hydrothermal circulation will tend to lower temperatures from that expected for a purely conductive cooling model (Fig. 4a). That said, local heating is possible through fluid redistributing heat within the crust. The minimum temperature limit within the crust is estimated assuming conductive heat transport within the sediment pile and efficient mixing in the crustal aquifer (i.e., a well mixed aquifer) leading to a constant temperature throughout the aquifer (Fisher and Becker, 2000)(Fig. 4a). Because of the slow sedimentation in both areas, and the early precipitation of calcite, the minimum temperature is roughly equal to bottom water temperature.

Figure 4a shows that the predicted range of temperatures within the crust bracket the calcite precipitation temperatures. The calcite precipitation temperature in the upper ~100 m of the Onophrious section, and the upper ~300 m of the Akaki section, match the minimum predicted temperature – that of Cretaceous bottom water. This indicates that these lava sections had sufficient recharge flux of cool seawater to efficiently extract the

ACCEPTED MANUSCRIPT

lithospheric heat and that the aquifer was thermally well mixed. Below these depths, calcite precipitation temperature increased ~0.1 $°Cm^{-1}$, suggesting the fluid was not thermally well mixed. Instead, this temperature gradient is equivalent to a conductive heat flux of 200 mWm^{-2} (assuming a thermal conductivity of 2 Wm^{-2} and that the calcites were precipitated synchronously). While this is a very rough approximation, this is the conductive heat flux predicted for 6.5 Myr old lithosphere (Stein and Stein, 1992). Thus, we interpret this temperature gradient as indicating that vertical fluid mixing at these depths (>100 m in Onophrious and >300 m in Akaki) did not lead to efficient heat transport. The increase in temperature with depth starting at ~100 m in the Onophrious section coincides with the transition from pillow to sheet flow dominated lava morphology (Fig. 1b) that would be expected to coincide with a decrease in vertical permeability within the crust. Similarly, although less strikingly, there is a substantial increase in the abundance of sheet flows below 300 m depth in the Akaki section. Thus, we interpret the different calcite precipitation temperature profiles as a function of depth in the Akaki and Onophrious sections to have been largely controlled by a difference in vertical permeability between these sections (Fig. 7). Sheet flows appear to have inhibited vertical mixing and likely led to both vertical and horizontal permeabilities that were lower than in pillow-dominated areas (Gillis and Sapp, 1997; Fisher, 1998).

In summary, within the upper zones where alteration occurred at near bottom water temperature and there are large CO_2 and alkali element enrichments, there must have been large fluxes of cold bottom water (Fig. 7). This requires high permeability consistent with these sections being dominated by pillow lavas. At greater depths, decreasing vertical permeability, due to an increase in the abundance of sheet flows, led

ACCEPTED MANUSCRIPT

to crustal temperatures increasing and the flux of fresh reactive fluid decreasing. Near conductive geotherms in these deeper regimes suggest vertical heat transport was largely conductive although horizontal fluid flow may have been important (e.g. Anderson et al., 2013). While the onset of sediment accumulation differed by ~20–30 Myr between areas, contrasting lava stratigraphies with differing permeability appears to be more important in fixing the hydrological regime in this very low sedimentation rate environment.

4.2. Comparison with modern ridge flanks – An evolving conceptual model for off-axis hydrothermal systems

With the aim of refining our understanding of how sedimentation history and crustal architecture influence the hydrological regime of the upper crust we compare the studied lava sections from the Troodos ophiolite to modern ridge flanks sampled by drilling. We consider how the timing of the onset of sedimentation, the rate of sedimentation, and the lithological make-up of the lava sections impact the hydrology and hence the thermal structure of the upper crust. We use carbonate formation temperature to estimate the thermal evolution of each crustal section although the time at which the crust achieved this temperature is not always well constrained (for temperature depth plots for the drill sites see Fig. 1, Anderson et al., 2013). Determining the reactive fluid flux through each crust section is more challenging. We use bulk-rock K_2O content as a proxy for the fresh reactive fluid flux because: (i) there is data for all drill sites (www.earthchem.org/petdb, Lehnert et al., 2000); (ii) K_2O generally tracks other geochemical tracers used to calculate fluid flux (e.g. this study; Staudigel et al., 1996); and (iii) the K content of seawater has stayed roughly constant throughout the

ACCEPTED MANUSCRIPT

Phanerozoic (Demicco et al., 2005). We use median K_2O values for all available data for each site as a proxy for fluid flux. Median K_2O values for altered cores that approximate the median global fresh mid-ocean ridge basalt (0.12 wt%, n > 7000, N-MORB samples with K_2O/TiO_2 <0.15, Melson et al., 2002) are considered to reflect low fluid fluxes, and incremental values higher than this are arbitrarily assigned moderate (0.2 to 0.3 wt%) and high (>0.5 wt%) fluid fluxes. We emphasize that these terms denote relative estimates of 'reactive fresh fluid' flux for comparative purposes only. The drill sites considered here have >100 m basement penetration and sufficient geochemical data to constrain temperature gradients and the extent of K_2O enrichment (Table 1). We exclude ODP Hole 801C due to evidence for off-axis magmatism at this site and Hole 1149D because the sedimentary section was not recovered.

The role of sedimentation history in controlling the hydrological regime in the crust is fairly clear in the drill core data. Sites with slow sedimentation rates (<3.5 m Myr^{-1}; the Akaki and Onophrious sections described above, and DSDP/ODP Holes 396B, 417A, 417D, 418A, 556, and 1224F) always have minimum carbonate precipitation temperatures similar to contemporaneous bottom seawater. Average carbonate precipitation temperatures are generally also similar to bottom water temperature in the upper portions of these holes although at depth, in the deeper holes, the temperature can increase substantially. In contrast, the fast-sedimentation sites (>30 m Myr^{-1}; ODP/IODP Sites 504B, 896A and 1256D) contain carbonates that almost all formed at temperatures above that of contemporaneous seawater, ranging up to 50–60°C at each site. We interpret this difference in carbonate formation temperature to reflect a combination of rapidly accumulating sediments both acting as a thermal blanket and inhibiting fluid

ACCEPTED MANUSCRIPT

entering and leaving the crust. For example, every 100 m of sediment will lead to a 10°C increase in basement temperature assuming a heat flux of 100 mW m^{-2} and a thermal conductivity of 1 $Wm^{-1}K^{-1}$. Furthermore, just a few 10's of m of sediment will act as an impermeable layer (Spinelli et al., 2004) preventing substantial ingress of cool seawater into the crust that, again, will lead to warmer basement temperatures. This interpretation of inhibited fluid fluxes at sites with rapid sedimentation rates is also consistent with the low bulk K_2O contents of all of these sites (<0.1 wt%; Table 1).

The role of crustal lithological architecture is more difficult to constrain from drill core data than that of sedimentation history because lithology is generally poorly quantified from drill cores with highly incomplete recovery. Because of this the Troodos sections described above perhaps provide the best insight into the role of crustal architecture in the hydrological regime. However the drill core data are consistent with the suggestion that increasing abundances of sheet flows inhibits fluid flow and hence decreases chemical exchange and increase crustal temperature. For example, Hole 417A which is 100% pillows except for the very basal unit, has a substantially higher K_2O content (~0.7 wt%) than Holes 471D or 418A (~0.1 wt%) which are comprised of intermixed pillows and sheet flows (~25%; Shipboard Scientific Party, 1979b; Donnelly et al., 1979; Flower et al., 1979; Staudigel et al., 1996). Unfortunately sedimentation started earlier at Holes 417D and 418A (Table 1) making it impossible to know whether the difference in sedimentation history or crustal architecture played the largest role in controlling the difference in extent of chemical exchange. The other site that appears to show evidence for the importance of sheet flow in inhibiting fluid flow in the crust is Hole 1256D. Here temperatures of carbonate precipitation increase progressively with

ACCEPTED MANUSCRIPT

depth (0.1°C m^{-1}) suggesting a thermally poorly mixed aquifer consistent with the sheet and massive flow dominated crustal stratigraphy and the scarcity of pillows in this section (Table 1).

Building on previous conceptual models for off-axis hydrothermal systems that considered how geological characteristics influence the hydrological regime of the upper crust (e.g. Fisher and Becker, 2000; Alt, 2004; Bach et al., 2004; Anderson et al., 2013), we use the analysis above and our new results from Troodos to place crustal alteration patterns into a hydrological framework (Fig. 7). At average, to below average, sedimentation rates, a regime that characterizes ~45% of the modern ocean basins, the upper crust alters within broad recharge/discharge zones as the crust initially moves away from the ridge axis (Fig. 7, left column). While these recharge zones may be focused at topographic highs (Hole 417A), more commonly they represent ambient (flattish) seafloor (Akaki, Holes 417D, 1224F, 556, 396B). This is because the crust remains hydrologically open until it is covered with a sufficient thickness (a few tens of metres; Spinelli et al., 2004) of low permeability sediment with some laterally continuity. Hydrological modeling predicts that the upper crust becomes locally hydraulically sealed within a few million years at global average sedimentation rates (3.5 m Myr^{-1}; Anderson et al., 2012). At lower sedimentation rates, such as those experienced in the Troodos ophiolite and the low sedimentation rate drill sites considered here, open exchange of seawater into and out of the crust could last several million years longer. The depth and intensity of the recharge signal reflects the duration of exposure (e.g. higher relative fluid fluxes at topographic high) and/or the lithological make-up of the crust (e.g. higher relative fluid fluxes associated with pillows). At high sedimentation rates (>20 m Myr^{-1}),

ACCEPTED MANUSCRIPT

such as those found at the equatorial Pacific drill sites, rapid sedimentation leads to low fluid fluxes and high temperatures within the aquifer (Fig. 7; right hand column). Recharge sites in these settings would be very short-lived and likely restricted to topographic highs. As these high sedimentation rates characterize <10% of the modern ocean basins, off-axis alteration at such sites is likely unrepresentative of average seafloor.

As the crust becomes sealed, outcrop-to-outcrop flow is initiated, shifting the flow of seawater in and out of the crust to seafloor topographic highs such as the crests of abyssal hills and seamounts. Between these zones, fluid flows laterally within the aquifer, warming due to conductive heat transfer into the base of the aquifer and the thermal insulation of the overlying sedimentary cover. The surface area of recharge/discharge sites decreases with crustal age (Anderson et al., 2012; Fisher and Becker, 2000), meaning that over time the bulk of the crust resides within lateral flow zones that undergo only minimal additional fluid-rock reaction. Using carbonate formation as an approximation of the cessation of alteration, lateral flow in crust >20 Myr old (e.g. Gillis and Coogan, 2011; Coogan and Dosso, 2015) would have minimal geochemical consequences.

5. Conclusions and implications

Two lava sections with contrasting sedimentation histories and lava stratigraphy in the well exposed Troodos ophiolite were studied to investigate how these parameters influence the evolution of off-axis, low temperature hydrothermal systems. The lava sections show significant compositional differences that reflect contrasting fluid fluxes

ACCEPTED MANUSCRIPT

and thermal regimes. The Akaki area is flat-lying and remained open to seawater recharge for 20–30 Myr whereas the Onophrious area formed in a small fault-bounded depression that was continuously sedimented from the time of crustal formation, albeit at very low sedimentation rates (<1 m Myr^{-1}). The upper lavas in both areas are enriched in CO_2, K_2O, Rb, Li, and $^{87}Sr/^{86}Sr$ with the Akaki section being more enriched than the Onophrious section. These upper enriched zones are composed of pillows and breccias in both areas; the enriched zone at Akaki is significantly thicker than at Onophrious (~300 m versus <100 m). The base of the enriched zones is marked by a change in lithology, to a mixture of pillows and sheet flows at Akaki and dominantly sheet flows at Onophrious. Overall, the Akaki section is 7 times more enriched in CO_2 and 3.5–4 times more enriched in K_2O, Rb, Li, and $^{87}Sr/^{86}Sr$ than the Onophrious section. The difference in extent of enrichment in the upper zones at Akaki and Onophrious, coupled with the difference in thickness, suggest the reactive fluid flux was much higher at Akaki than at Onophrious. Calcite precipitation temperatures determined from O-isotope thermometry are similar to contemporaneous seawater in the upper pillow-dominated zones in both areas, and increased to ~35°C within the lower lavas. Collectively, these trends suggest the crustal aquifer was well mixed in the upper enriched zones, but became poorly mixed with depth due to changes in the lithological make-up of the lava pile. The lithological make-up of the lava sections appears to be more important than the contrasting sedimentation histories, likely due to the very low sedimentation rate in both areas (<1 m Myr^{-1}).

The altered lavas are enriched in δ^7Li, with the upper enriched zone at Akaki being slightly heavier (~3‰) than lavas deeper in the section and all but one sample from

ACCEPTED MANUSCRIPT

the Onophrious section. The heavier samples (9.5–12‰) are more K_2O-rich than the lighter samples (7–9‰), suggesting the bulk fractionation factor may be dependent on the secondary mineral assemblage, with the more-K-rich clay minerals having smaller fractionation factors.

The conceptual model for off-axis hydrothermal systems shown in Figure 7 suggests that hydrothermal flow and reaction in ridge flanks cannot be a uniform process that proceeds simply as a function of crustal age due to diminishing heat flux and increasing sediment thickness. Rather, regional variations in sedimentation rate, the timing of the onset of accumulation of an impermeable sedimentary cover, and crustal architecture result in significant lateral variation in the extent of ocean–crust chemical exchange and the thermal regime within the crust. This has significant implications for quantifying global geochemical fluxes, and understanding the impact of ocean-crustal chemical exchange on ocean chemistry and subduction zone inputs. Fluxes associated with different hydrological regimes, and the relative proportions of each regime globally, will need to be quantified to determine global chemical fluxes. Moreover, it cautions against extrapolating globally geochemical fluxes calculated for high sedimentation rate hydrological regimes that are easier to drill into, but are globally unrepresentative.

ACCEPTED MANUSCRIPT

Acknowledgements

We acknowledge the Cyprus Geological Survey Department for storing the ICRDG drillcores and providing access to the international community. We thank the following colleagues for their analytical assistance: J. Spence (ICP-MS), M. Raudsepp (Electron microprobe), J. Gabites (O-isotopes), and B. Keiffer (Sr-isotopes). P. Luck and M. Burns contributed to collection of glass and mineral compositions, respectively. We also thank M. Regelous, two anonymous reviewers, and Editor-in-chief C. Chauvel for their constructive reviews. Field and analytical work was supported by NSERC Discovery grants to LAC and KMG.

ACCEPTED MANUSCRIPT

ACCEPTED MANUSCRIPT

Figure captions:

Figure 1. Simplified geological maps and lithological columns for the (a) Akaki and (b) Onophrious River sections (both rivers flow to the north). Depth distribution of lithologies for Akaki is based on the CY1/1a drillcore (Gibson et al, 1991), which is very similar to surface outcrops (e.g. Rautenschlein et al., 1985). (c) Map of Cyprus showing the locations of Troodos ophiolite (grey) and Akaki and Onophrious River sections.

Figure 2. Whole rock CO_2, K_2O, Rb, and Li contents versus depth below the sediment-lava contact. The black symbols show average values for 50 m depth intervals (symbols centred mid-way within each interval). Grey areas indicate the range for fresh glass values from the combined study areas (Supplementary Table 2; Regelous et al., 2014). Published Hole CY-1/1A data from Gibson et al. (1991); these data were collected by XRF.

Figure 3. (a) Age corrected whole rock $^{87}Sr/^{86}Sr$ versus depth below the sediment-lava contact. The grey line (left) shows the average fresh rock value and grey area (right) indicates the range for 70–90 Ma seawater. (b) Age corrected whole rock $^{87}Sr/^{86}Sr$ versus Sr contents. Contour lines show *reactive* water-rock ratios, calculated assuming a fresh-rock starting point (90 ppm Sr, 0.7035), seawater Sr content = 20 ppm, seawater $^{87}Sr/^{86}Sr$ = 0.7074, and hydrothermal fluid = 0.70735 (from calcite). The zero *reactive* water-rock ratio contour is shown to guide the eye and reflects simple precipitation of seawater Sr into the rock with no rock dissolution and thus no change in fluid Sr isotopic composition. See Appendix A for whole rock age correction details and the equations for calculation of the water-

ACCEPTED MANUSCRIPT

rock ratio curves. Data sources: this study; Gillis and Robinson (1990). The uncertainty of the Sr-isotope and Sr concentrations fall within the size of the symbols used.

Figure 4. (a) Calculated formation temperatures of calcite separates versus depth below the sediment-lava contact. The dashed black lines represent a purely conductive geothermal gradient at 5 and 20 Myr after crustal formation, calculated using the heat flow model of Stein and Stein (1994), and solid black line represents the geothermal gradient for a well-mixed aquifer (see text for details). (b) Calcite $^{87}Sr/^{86}Sr$ versus depth below the sediment-lava contact. Dashed lines indicate the $^{87}Sr/^{86}Sr$ of seawater at 70, 80, and 90 Ma (McArthur et al., 2001).

Figure 5. (a) Whole rock δ^7Li depth below the sediment-lava contact Li versus δ^7Li. Samples in the low K_2O (<1.01 wt%; solid line) and high K_2O (>1.5 wt%, dashed line) groups have ≥14 ppm Li. Error bars for δ^7Li are ± 1. 5‰, the uncertainty of Li concentrations lies within the size of the symbols.

Figure 6. (a) K_2O, (b) Rb, and (c) Li contents versus total Al for clay minerals. K-rich clay minerals (celadonite, celadonite-saponite mixtures) are also enriched in Rb, but show lower Li than the K-poor clay minerals (Al-saponite, saponite, saponite-chlorite mixtures). Major element mineral compositions were recalculated on the basis of 22 anhydrous oxygens.

Figure 7. Conceptual model for the thermal and geochemical evolution of off-axis hydrothermal systems at different sedimentation rates. (left) Low to average sedimentation rates: As a crustal section initially migrates off-axis (Time 1), cold bottom water flows freely into and out of the crustal aquifer, leading to high

ACCEPTED MANUSCRIPT

reactive fluid fluxes and chemical exchange particularly in the uppermost lavas. As an impermeable sedimentary cover accumulates (Time 2), points of recharge/discharge become focused at topographic highs, leading to localized high fluxes of reactive fluid flow and continued reaction at recharge sites. By the time the aquifer is hydrologically sealed (Time 3), reactive fluid flow and concomitant reaction has largely ceased; temperatures recorded in carbonates are equivalent to bottom seawater throughout the lava pile where pillows dominate and increase with depth where the lithologies are mixed with, or dominated by, sheet flows. (right) High sedimentation rates: The progression from open chemical exchange to the aquifer being sealed from the ingress of reactive fluids is highly compressed in time, and is largely complete by Time 2. This results in far less chemical exchange and higher aquifer temperatures (Time 3). Ellipses = pillows/breccias, horizontal lines = sheet/massive flows, grey shade = sediment cover. The horizontal temperature scales for the temperature (T) – depth plots shown in panels for Time 3 are from 0 to 60°C and reflect the temperature during the main stage of reactive fluid flow and geochemical exchange. Stippled areas (black dots) identify areas of moderate to high enrichment of K_2O and Sr-isotopes, used as a proxy for the reactive fluid flux. Blue arrows depict the flow of cold reactive fresh fluid; line thicknesses represent the relative magnitude of fluid fluxes.

ACCEPTED MANUSCRIPT

References:

Alt, J.C., 2004. Alteration of the upper oceanic crust: mineralogy, chemistry and processes. In: Davis, E.E., Elderfield, H. (Eds.), Hydrogeology of the Oceanic Lithosphere. Cambridge University Press, Cambridge, pp. 495-533.

Anderson, B.W., Coogan, L.A., Gillis, K.M., 2012. The role of outcrop-to-outcrop fluid flow in off-axis oceanic hydrothermal systems under abyssal sedimentation conditions. J. Geophys. Res., 117.

Anderson, B.W., Gillis, K.M., Coogan, L.A., 2013. A hydrologic model for the uppermost oceanic crust constrained by temperature estimates from carbonate minerals. J. Geophys. Res., 118(8): 3917-3930.

Bach, W., Humphris, S.E., Fisher, A.T., 2004. Fluid flow and fluid-rock interaction within ocean crust: reconciling geochemical, geological, and geophysical observation. In: Wilcock, W.S.D., DeLong, E.F., Kelley, D.S., Baross, J.A., Cary, S.C. (Eds.), The Subseafloor Biosphere at Mid-ocean Ridges. Geophysical Monograph v. 144. Amer. Geophys. Un., Washington, DC, pp. 99-117.

Bear, L.M., 1960. The geology and mineral resources of the Akaki-Lythrodondha area. Cyprus Geological Survey Department Memoir 3. Government of Cyprus, Nicosia, 122 pp.

Bednarz, U., Schmincke, H.-U., 1989. Mass transfer during sub-seafloor alteration of the upper Troodos crust (Cyprus). Contrib. Mineral. Petrol., 102: 93-101.

Booij, E., Gallahan, W.E., Staudigel, H., 1995. Ion-exchange experiments and Rb/Sr dating on celadonites from the Troodos ophiolite, Cyprus. Chem. Geol., 126: 155-167.

ACCEPTED MANUSCRIPT

Brady, P.V., Gislason, S.R., 1997. Seafloor weathering controls on atmospheric CO_2 and global climate. Geochim. Cosmochim. Acta, 61: 965-973.

Chan, L.H., Alt, J.C., Teagle, D.A.H., 2002. Lithium and lithium isotope profiles through the upper oceanic crust: a study of seawater-basalt exchange at ODP Sites 504B and 896A. Earth Planet. Sci. Lett., 201(1): 187-201.

Chan, L.H., Edmond, J.M., Thompson, G., Gillis, K., 1992. Lithium isotopic composition of submarine basalts: implications for the lithium cycle in the oceans. Earth Planet. Sci. Lett., 108: 151-160.

Coggon, R.M., Teagle, D.A.H., Smith-Duque, C.E., Alt, J.C., Cooper, M.J., 2010. Reconstructing Past Seawater Mg/Ca and Sr/Ca from Mid-Ocean Ridge Flank Calcium Carbonate Veins. Science, 327(5969): 1114-1117.

Coogan, L.A., Dosso, S.E., 2015. Alteration of ocean crust provides a strong temperature dependent feedback on the geological carbon cycle and is a primary driver of the Sr-isotopic composition of seawater. Earth Planet. Sci. Lett., 415: 38-46.

Coogan, L.A., Gillis, K.M., 2013. Evidence that low-temperature oceanic hydrothermal systems play an important role in the silicate-carbonate weathering cycle and long-term climate regulation. Geochem. Geophys. Geosys., 14(6): 1771-1786.

Demicco, R.V., Lowenstein, T.K., Hardie, L.A., Spencer, R.J., 2005. Model of seawater composition for the Phanerozoic. Geology, 33(11): 877-880.

Donnelly, T.W., Pritchard, R.A., Emmermann, R., Puchelt, H., 1979. The aging of oceanic crust: synthesis of the mineralogical and chemical results of Deep Sea Drilling Project, Legs 51 through 53. In: Donnelly, T., Francheteau, J., Bryan, W.,

ACCEPTED MANUSCRIPT

Robinson, P., Flower, M., Salisbury, M. (Eds.), Init. Repts. DSDP, v. 51, 52, 53. U.S. Government Printing Office, Washington, D.C., pp. 1563-1577.

Eggins, S.M., Woodhead, J.D., Kinsley, L.P.J., Mortimer, G.E., Sylvester, P., McCulloch, M.T., Hergt, J.M., Handler, M.R., 1997. A simple method for the precise determination of ≥40 trace elements in geological samples by ICPMS using enriched isotope internal standardisation. Chem. Geol., 134: 311-326.

Fisher, A.T., 1998. Permeability within basaltic oceanic crust. Rev. Geophys., 36(2): 143-182.

Fisher, A.T., Becker, K., 2000. Channelized fluid flow in oceanic crust reconciles heat-flow and permeability data. Nature, 403: 71-74.

Fisher, A.T., Wheat, C.G., 2010. Seamounts as conduits for massive fluid, heat, and solute fluxes on ridge flanks. Oceanography, 23(1): 74-87.

Flower, M.F.J., Ohnmacht, W., Robinson, P.T., Marriner, G., Schmincke, H.-U., 1979. Lithologic and chemical stratigraphy at Deep Sea Drilling Project Sites 417 and 418. In: Donnelly, T., Francheteau, J., Bryan, W., Robinson, P., Flower, M., Salisbury, M. (Eds.), Init. Rept., DSDP, v. 51, 52, 53. U.S. Priniting Office, Washington, pp. 939-956.

Francois, L.M., Walker, J.C.G., 1992. Modelling the Phanerozoic carbon cycle and climate: constraints from the $^{87}Sr/^{86}Sr$ isotopic ratio of seawater. Amer. J. Sci., 292: 81-135.

Friedmann, I., O'Neil, J.R., 1977. Compliation of stable isotope fractionation factors of geological interest. In: Fleischer, M. (Ed.), Data of Geochemistry. Geol. Surv. Prof. Paper 440-KK, Reston, VA, 117 pp.

ACCEPTED MANUSCRIPT

Gallahan, W.E., Duncan, R.A., 1994. Spatial and temporal variability in crystallization of celadonites within the Troodos ophiolite, Cyprus: Implications for low-temperature alteration of the oceanic crust. J. Geophys. Res., 99: 3147-3161.

Gibson, I.L., Malpas, J., Robinson, P.T., Xenophontos, C. (Eds.), 1991. Cyprus Crustal Study Project: Initial reports, Holes CY1 and 1a. Geological Survey of Canada Paper, 90-20, Ottawa, 283 pp.

Gillis, K.M., Coogan, L.A., 2011. Secular variation in carbon uptake into the ocean crust. Earth Planet. Sci. Lett., 302(3-4): 385-392.

Gillis, K.M., Robinson, P.T., 1988. Distribution of alteration zones in the upper oceanic crust. Geol., 16: 262-266.

Gillis, K.M., Robinson, P.T., 1990. Patterns and processes of alteration in the lavas and dykes of the Troodos Ophiolite, Cyprus. J. Geophys. Res., 95: 21,523-21,548.

Gillis, K.M., Sapp, K., 1997. Distribution of porosity in a section of upper oceanic crust exposed in the Troodos Ophiolite. J. Geophys. Res., 102(B5): 10133-10149.

Hart, S.R., Staudigel, H., 1982. The control of alkalies and uranium in seawater by ocean crust alteration. Earth Planet. Sci. Lett., 58: 202-212.

Higgins, J.A., Schrag, D.P., 2015. The Mg isotopic composition of Cenozoic seawater – evidence for a link between Mg-clays, seawater Mg/Ca, and climate. Earth Planet. Sci. Lett., 416(0): 73-81.

Huber, B.T., Norris, R.D., MacLeod, K.G., 2002. Deep-sea paleotemperature record of extreme warmth during the Cretaceous. Geol., 30(2): 123-126.

ACCEPTED MANUSCRIPT

Jochum, K. P., Nohl, L., Herwig, K., Lammel, E., Stoll, B., and Hofmann, A. W., 2005, GeoReM: A new geochemical database for reference materials and isotopic standards. Geostand. Geoanal. Res. 29(3): 333-338.

Krasheninnikov, V.A., 1979. Stratigraphy and planktonic foraminifers of Neogene and Quaternary sediments of Site 396, Leg 46 of DSDP. In: Dmitriev, L., Heirtzler, J., (Eds.), Init. Rept., DSDP, v. 46. U.S. Priniting Office, Washington, pp. 409-413.

Lehnert, K., Su, Y., Langmuir, C., Sarbas, B., Nohl, U., 2000. A global geochemical database structure for rocks. Geochem. Geophys. Geosyst., 1.

Magna, T., Wiechert, U., Grove, T.L., Halliday, A.N., 2006. Lithium isotope fractionation in the southern Cascadia subduction zone. Earth Planet. Sci. Lett., 250(3-4): 428-443.

McArthur, J.M., Howarth, R.J., Bailey, T.R., 2001. Strontium isotope stratigraphy: LOWESS version 3: Best fit to the marine Sr-isotope curve for 0-509 Ma and accompanying look-up table for deriving numerical age. J. Geol., 109(2): 155-170.

Melson, W.G., O'Hearn, T., Jarosewich, E., 2002. A data brief on the Smithsonian Abyssal Volcanic Glass Data File. Geochem. Geophys. Geosys., 3.

Misra, S., Froelich, P.N., 2012. Lithium isotope history of Cenozoic seawater: Changes in silicate weathering and reverse weathering. Science, 335(6070): 818-823.

Miyashiro, A., 1973. The Troodos ophiolitic complex was probably formed in an island arc. Earth Planet. Sci. Lett., 19: 218-224.

ACCEPTED MANUSCRIPT

Mottl, M.J., Wheat, C.G., 1994. Hydrothermal circulation through mid-ocean ridge flanks: Fluxes of heat and magnesium. Geochim. Cosmochim. Acta, 58: 2225-2237.

Mukasa, S.B., Ludden, J.N., 1987. Uranium-lead isotopic ages of plagiogranites from the Troodos ophiolite, Cyprus and their tectonic significance. Geol., 15: 825-828.

Rausch, S., Bohm, F., Bach, W., Klugel, A., Eisenhauer, A., 2013. Calcium carbonate veins in ocean crust record a threefold increase of seawater Mg/Ca in the past 30 million years. Earth Planet. Sci. Lett., 362: 215-224.

Rautenschlein, M., Jenner, G.A., Hertogen, J., Hofmann, A.W., Kerrich, R., Schmincke, H.-U., White, W.M. 1985. Isotopic and trace element composition of volcanic glasses from the Akaki Canyon, Cyprus: implications for the origin of the Troodos ophiolite. Earth Planet. Sci. Lett., 75: 369-383.

Regelous, M., Haase, K.M., Freund, S., Keith, M., Weinzierl, C.G. Beier, C., Brandl, P.A., Endres, T., Schmidt, H., 2014. Formation of the Troodos Ophiolite at a triple junction: Evidence from trace elements in volcanic glass. Chem. Geol., 386: 66-79.

Shipboard Scientific Party, 1979a. Site 417. In: Donnelly, T., Francheteau, J., Bryan, W., Robinson, P., Flower, M., Salisbury, M. (Eds.), Init. Rept., DSDP, v. 51, 52, 53. U.S. Priniting Office, Washington, DC, pp. 23-350.

Shipboard Scientific Party, 1979b. Site 418. In: Donnelly, T., Francheteau, J., Bryan, W., Robinson, P., Flower, M., Salisbury, M. (Eds.), Init. Rept. DSDP, v. 51, 52, 53. U.S. Govt. Printiing Office, Washington, DC, pp. 351-626.

ACCEPTED MANUSCRIPT

Shipboard Scientific Party, 1985. Site 556. In: Bougalt, H., Cande, S.C., et al., (Eds.), Init. Rept., DSDP, v. 82. U.S. Printing Office, Washington, DC, pp. 61-113.

Shipboard Scientific Party, 1993. Site 896. In: Alt, J.C., Kinoshita, H., Stokking, L.B. (Eds.), Proc. ODP, Sci. Results, v. 148. Ocean Drilling Program, College Station, TX, pp. 123-192.

Spinelli, G.A., Giambalvo, E.R., Fisher, A.T., 2004. Sediment permeability, distribution, and influence on fluxes in oceanic basement. In: Davis, E.E., Elderfield, H. (Eds.), Hydrogeology of the Oceanic Lithosphere. Cambridge Univ. Press, Cambridge, UK, pp. 151-188.

Spooner, E.T.C., Chapman, H.J., Smewing, J.D., 1977. Strontium isotopic contamination and oxidation during ocean floor hydrothermal metamorphism of the ophioliteic rocks of the Troodos Massif, Cyprus. Geochim. Cosmochim. Acta, 41: 873-890.

Staudigel, H., 2014. 4.16 - Chemical Fluxes from Hydrothermal Alteration of the Oceanic Crust. In: Turekian, H.D.H.K. (Ed.), Treatise on Geochemistry (Second Edition). Elsevier, Oxford, pp. 583-606.

Staudigel, H., Gillis, K., Duncan, R., 1986. K/Ar and Rb/Sr ages of celadonites from the Troodos ophiolite, Cyprus. Geol., 14(1): 72-75.

Staudigel, H., Gillis, K.M., 1990. The timing of hydrothermal alteration in the Troodos Ophiolite. In: Malpas, J., Moores, E.M., Panayiotou, A., Xenophontos, C. (Eds.), Ophiolites: Oceanic crust analogues, Proceeding of the symposium "Troodos 1987". Geological Survey Department, Nicosia, pp. 665-672.

Staudigel, H., Plank, T., White, B., Schimincke, H.-U., 1996. Geochemical fluxes during seafloor alteration of the basaltic upper oceanic crust: DSDP Sites 417 and 418.

ACCEPTED MANUSCRIPT

In: Bebout, G.E., Scholl, D.W., Kirby, S.H., Platt, J.P. (Eds.), Subduction: Top to bottom. Geophys. Mono. V. 46, Amer. Geophys. Un., Washington, DC, pp. 19-38.

Stein, C.A., Stein, S., 1992. A model for the global variation in oceanic depth and heat flow with lithospheric age. Nature, 359: 123-137.

Stein, C.A., Stein, S., 1994. Constraints on hydrothermal heat flux through the oceanic lithosphere from global heat flow. J. Geophys. Res., 99: 3081-3095.

Stroncik, N.A., Schmincke, H.U., 2001. Evolution of palagonite: Crystallization, chemical changes, and element budget. Geochem. Geophys. Geosys., 2.

Teagle, D.A.H., Alt, J.C., Bach, W., Halliday, A.N., Erzinger, J., 1996. Alteration of upper ocean crust in a ridge-flank hydrothermal upflow zone: Mineral, chemical, and isotopic constraints from Hole 896A. In: Alt, J.C., Kinoshita, H., Stokking, L.B., Michaels, P.J. (Eds.), Proc. ODP, Sci. Results. Ocean Drilling Program, College Station, TX, pp. 119-150.

Teppen, B.J., Miller, D.M., 2006. Hydration energy determines isovalent cation exchange selectivity by clay minerals. Soil Science Soc. Amer. J., 70(1): 31-40.

Tomascak, P.B., Langmuir, C.H., le Roux, P.J., Shirey, S.B., 2008. Lithium isotopes in global mid-ocean ridge basalts. Geochim. Cosmochim. Acta, 72(6): 1626-1637.

Tomascak, P.B., Widom, E., Benton, L.D., Goldstein, S.L., Ryan, J.G., 2002. The control of lithium budgets in island arcs. Earth Planet. Sci. Lett., 196(3-4): 227-238.

Tominaga, M., Teagle, D.A.H., Alt, J.C., Umino, S., 2009. Determination of the volcanostratigraphy of oceanic crust formed at superfast spreading ridge:

ACCEPTED MANUSCRIPT

Electrofacies analyses of ODP/IODP Hole 1256D. Geochem. Geophys. Geosys., 10.

Veizer, J. et al., 1999. $^{87}Sr/^{86}Sr$, $\delta^{18}O$ evolution of Phanerozoic seawater. Chem. Geol., 161: 59-88.

Vigier, N. et al., 2008. Quantifying Li isotope fractionation during smectite formation and implications for the Li cycle. Geochim. Cosmochim. Acta, 72(3): 780-792.

ACCEPTED MANUSCRIPT

ACCEPTED MANUSCRIPT

Table 1. Summary of the site characteristics for the DSDP/ODP/IODP holes discussed

Hole[a]	Crustal age	Sedimentation rate[b]	Lithostrat. (decreasing order of abundance)[c]	Median K_2O (wt%)[d]	n	Average T °(C)[e] ± 1 s.d.	n	Temperature gradient (°C/m)[f]
396B	13.4	<1 for 14-5.3 Ma, 26 for 5.3 to present[f]	Pillows, breccias	0.21	181	2 ± 1	16	N
417A	119	5.3 for 100-66 Ma, 0.9 for 66 Ma to present	Pillows, hyaloclastic breccia (20%), massive flow	0.67	62	21 ± 5	47	N
417D	119	0.25 for 119-100 Ma, 5.3 for 100-66 Ma, 0.9 for 66 Ma to present	Pillows, minor massive flow, pillow breccia (6%)	0.08	189	22 ± 9	27	N
418A	119	0.25 for 119-100 Ma, 5.3 for 100-66 Ma, 0.9 for 66 Ma to present	Pillows, pillow breccia (6%), massive flows	0.08	302	36 ± 17	20	0.1
504B	6.9	34 for 6.9-5.4 Ma, 36 for 5.4-3.7 Ma, 50 for 3.7-1.9 Ma, 40 for 1.9-0.9 Ma, 25 for 0.9 Ma to present	Pillows (57%), massive (22%) and thin flows (17.5%)	0.08	409	32 ± 17	7	N
556	31	1 for 31-16.4 Ma, 29 for 16.4 Ma to present	Breccias, pillows, gabbroic breccia	0.25	91	7 ± 2	23	0.06
896A	6.9	Same as 504B	Pillows (57%), massive flows (38%), breccia (5%)	0.10	235	43 ± 14	25	Bi-modal
1224F	46	8 for 45-42 Ma, 0.1 for 42Ma to present[g]	Massive flow capping section, pillows	0.30	72	6 ± 2	18	N
1256D	14	44.5 for 15-11.2 Ma, 2.5 for 11.2-3.8 Ma, 9.7 for 3.8 Ma to present	Fragmented flows (32%), massive flows (22%), breccias (19%), pillows (1.9%)	0.05	53	61 ± 12	21	0.1

[a] See Supplementary Figure 1 for locations.
[b] From compilation in Anderson et al. (2013); Hole 396B data from Krasheninnikov (1979)
[c] Data from compilation in Gillis and Coogan (2011); Hole 1256D data from Tominaga et al., (2009)
[d] Data compiled using www.earthchem.org/petdb, Lehnert et al. (2000); additional Hole 896A data from Teagle et al. (1996)
[e] Data from compilation in Gillis and Coogan (2011) and Rausch et al. (2013)
[f] N = No gradient
[g] Poorly constrained sedimentation rates

ACCEPTED MANUSCRIPT

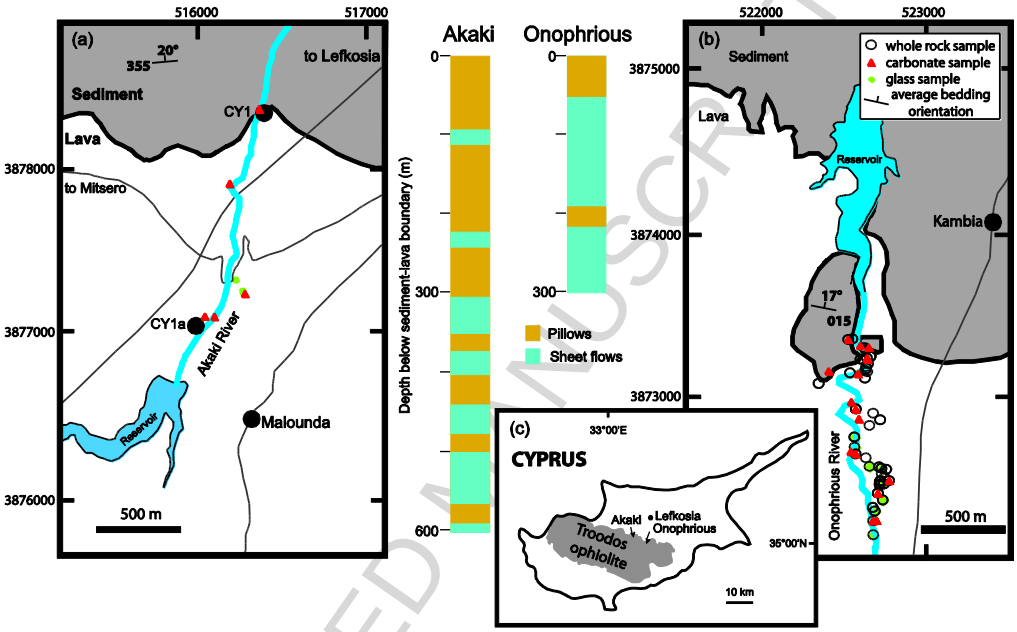

Figure 1 (two columns)

ACCEPTED MANUSCRIPT

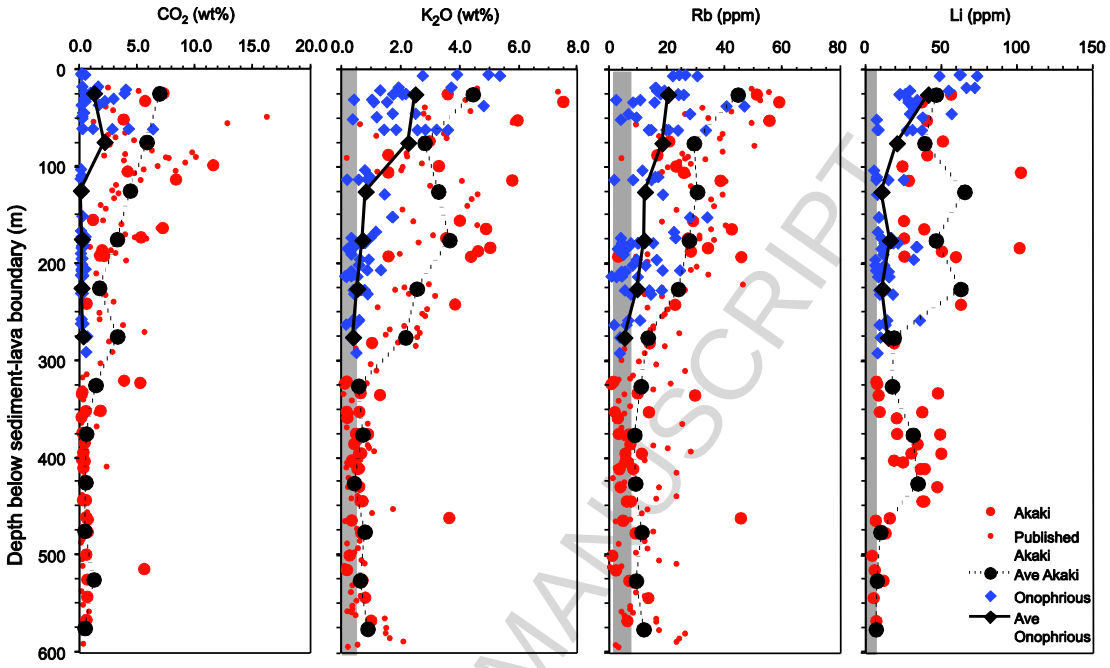

Figure 2

ACCEPTED MANUSCRIPT

ACCEPTED MANUSCRIPT

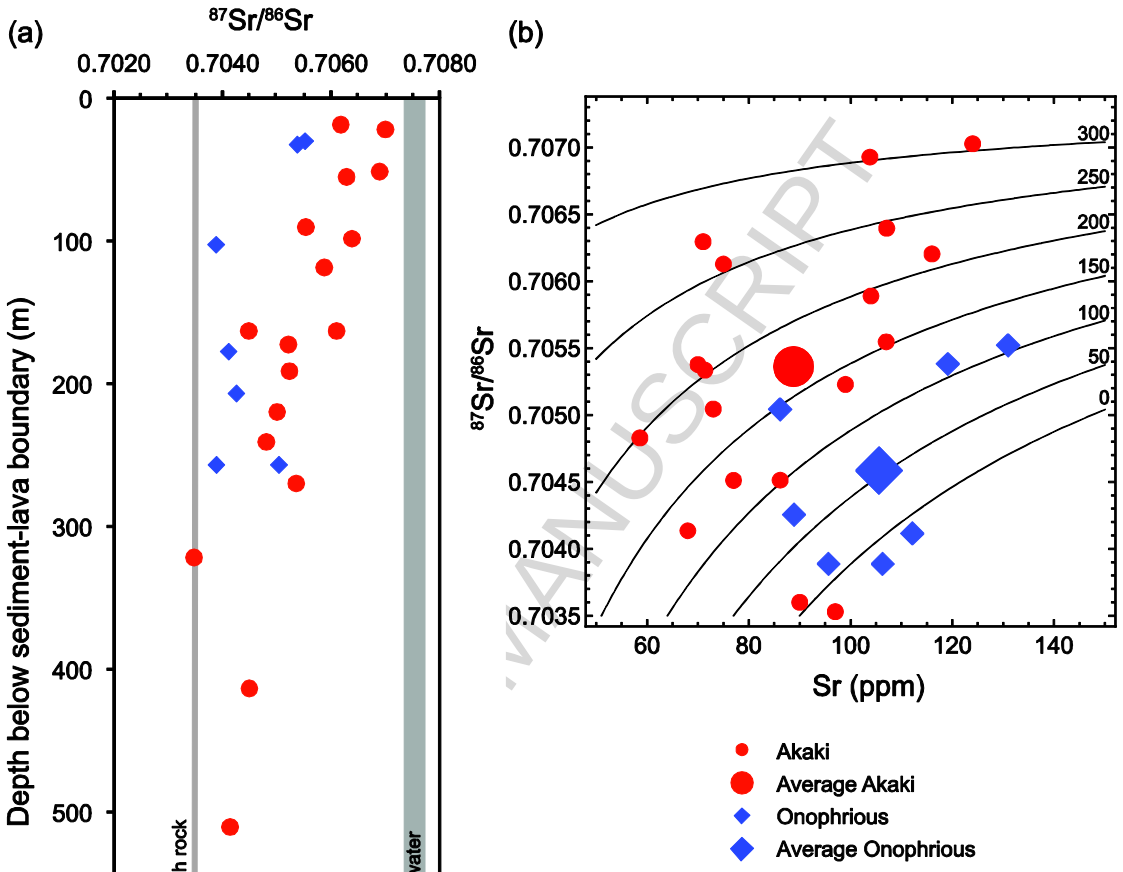

Figure 3 (1.5 columns)

ACCEPTED MANUSCRIPT

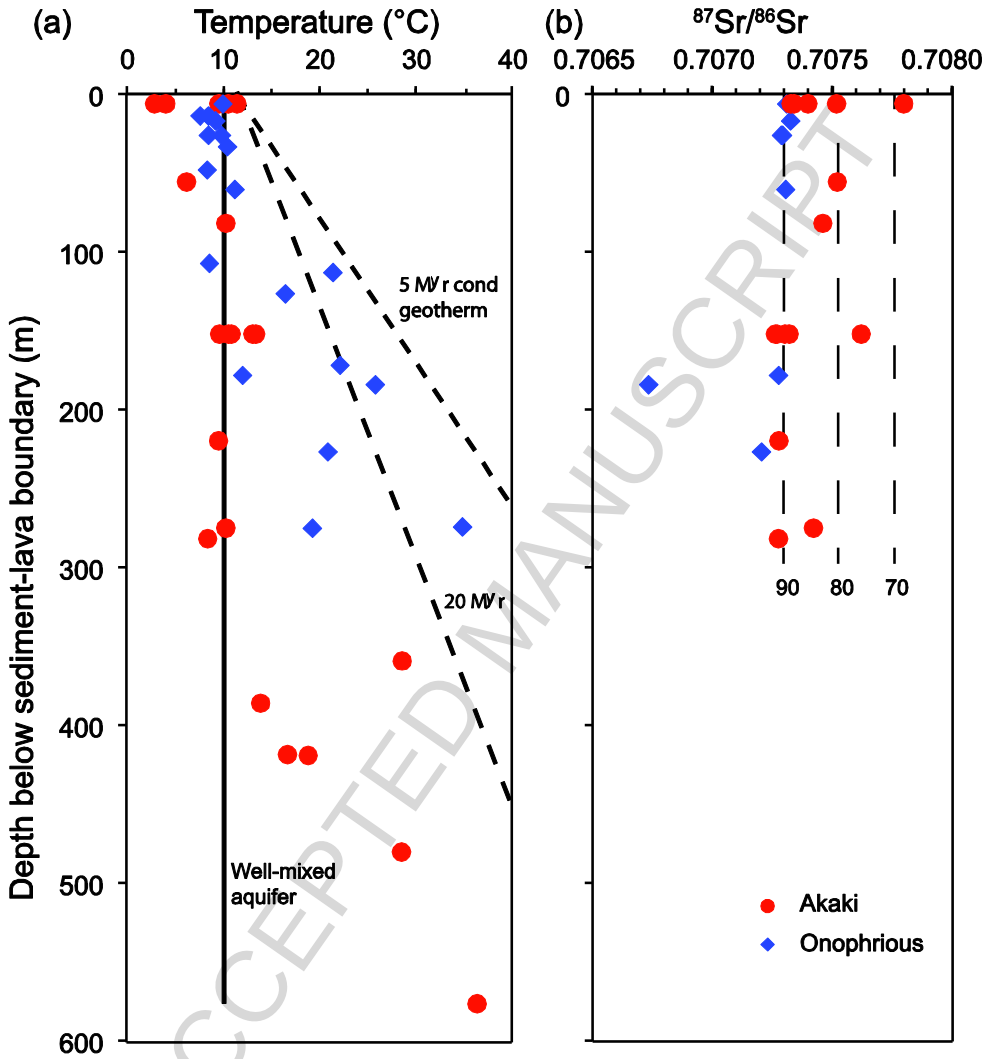

Figure 4 (1.5 columns)

ACCEPTED MANUSCRIPT

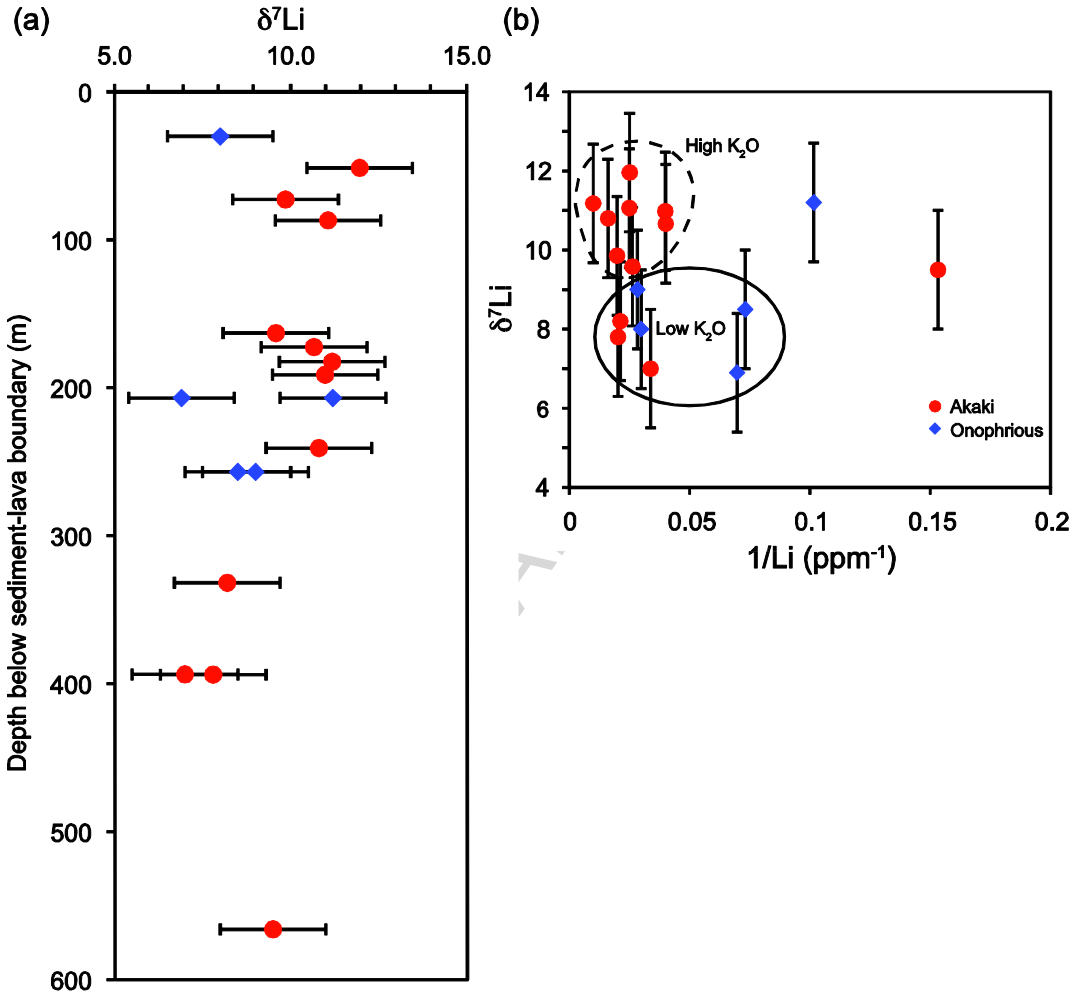

Figure 5 (1.5 columns)

ACCEPTED MANUSCRIPT

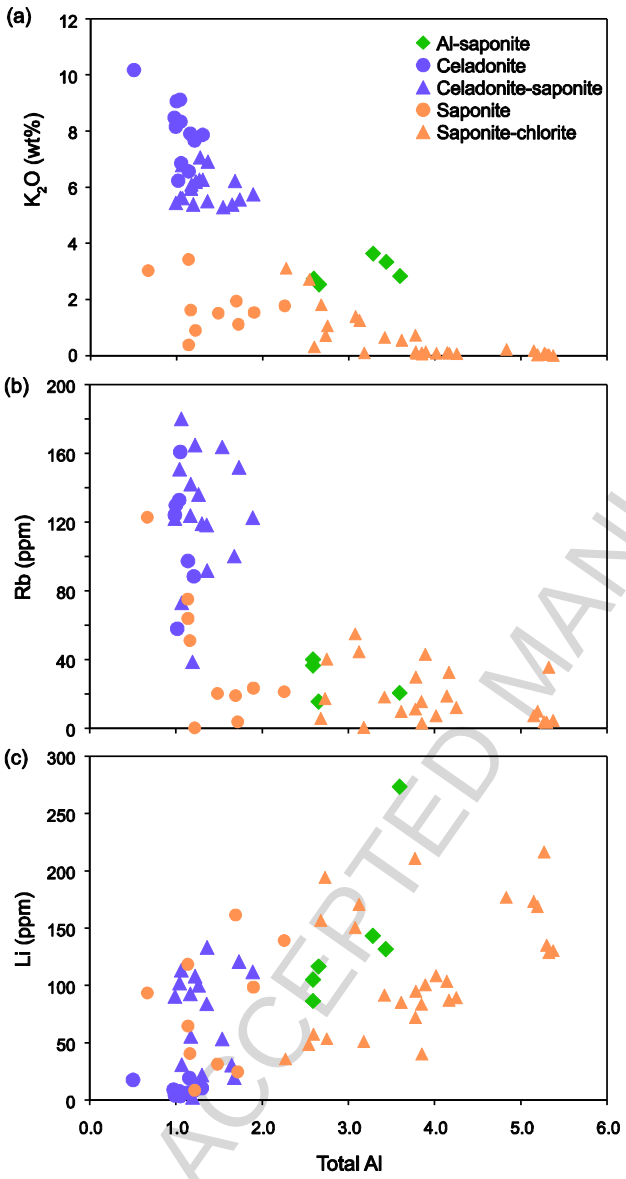

Figure 6

ACCEPTED MANUSCRIPT

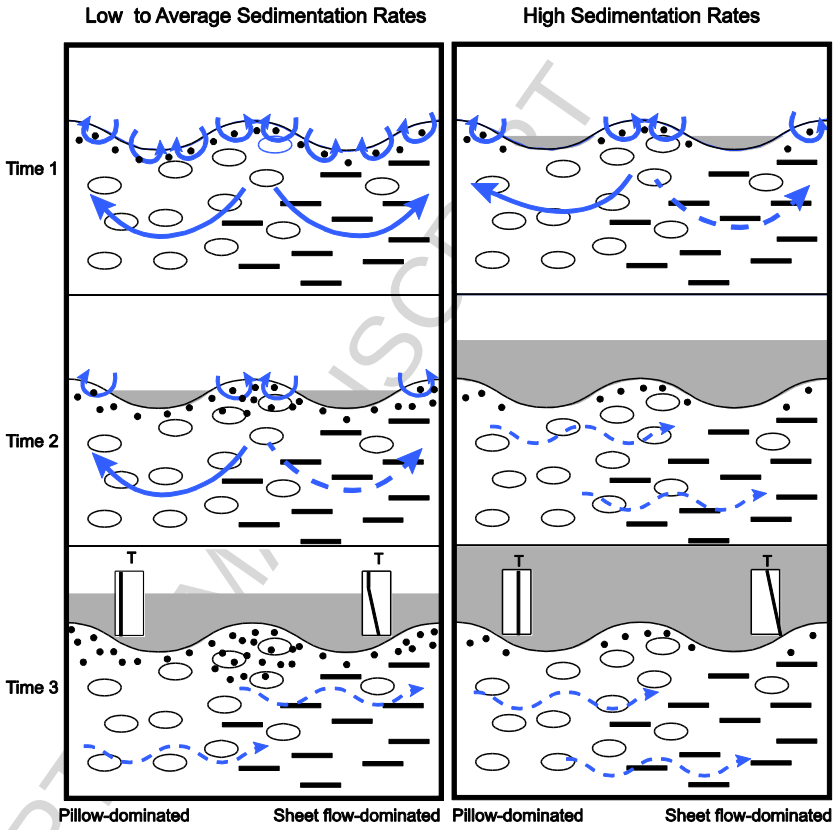

Figure 7 (2 columns)

ACCEPTED MANUSCRIPT

Highlights:

• Two lava sections from the Troodos ophiolite show contrasting enrichment in CO_2, alkali elements, and Sr- and Li-isotopes

• The two lava sections show contrasting calcite formation temperature depth profiles

• Chemically enriched lava section records higher reactive fluid fluxes in a cold crustal aquifer

• Off-axis hydrothermal systems have significant lateral variation in the extent of ocean-crust exchange and thermal regime

• Sedimentation history and crustal architecture are important controls on off-axis hydrothermal fluxes

ACCEPTED MANUSCRIPT